IOP Publishing Plasma Physics and Controlled Fusion
Plasma Phys. Control. Fusion **62** (2020) 045013 (8pp) https://doi.org/10.1088/1361-6587/ab7608

Growth rate and gain of stimulated Brillouin scattering considering nonlinear Landau damping due to particle trapping

Q S Feng[1], L H Cao[1,2,3,4], Z J Liu[1,2], L Hao[1], C Y Zheng[1,2,3,4], C Ning[1] and X T He[1,2,3]

[1] Institute of Applied Physics and Computational Mathematics, Beijing, 100094, People's Republic of China
[2] HEDPS, Center for Applied Physics and Technology, Peking University, Beijing 100871, People's Republic of China
[3] Collaborative Innovation Center of IFSA (CICIFSA) , Shanghai Jiao Tong University, Shanghai, 200240, People's Republic of China

E-mail: cao_lihua@iapcm.ac.cn and zheng_chunyang@iapcm.ac.cn

Received 18 September 2019, revised 6 February 2020
Accepted for publication 13 February 2020
Published 26 February 2020

Abstract

Growth rate and gain of stimulated Brillouin scattering (SBS) considering the reduced Landau damping due to particle trapping has been proposed to predict the growth and average level of SBS reflectivity. Due to particle trapping, the reduced Landau damping has been taken used of to calculate the gain of SBS, which will make the simulation data of SBS average reflectivity be consistent to the Tang model better. Other nonlinear effects such as harmonic generation and pump depletion have been also considered in the later evolution of SBS. This work may solve the pending questions in laser-plasma interaction and have wide applications in parametric instabilities.

Keywords: stimulated Brillouin scattering, ion acoustic waves, inertial confinement fusion, laser plasma interaction

(Some figures may appear in colour only in the online journal)

1. Introduction

Backward stimulated Brillouin scattering (SBS) is a three-wave interaction process where an incident electromagnetic wave (EMW) decays into a backscattered EMW and a forward propagating ion-acoustic wave (IAW), which will lead to a great energy loss of the incident laser and is detrimental in inertial confinement fusion (ICF) [1–3]. In the indirect-drive ICF [2, 3] or the hybrid-drive ignition [1, 4–6], CH was chosen as the standard ablator material for ICF ignition capsules due to its low atomic number, high density, and a host of manufacturing considerations. Thus, the inside of hohlraum will be filled with low-Z plasmas, such as H or CH plasmas from the initial filled material or from the ablated material off the capsule.

It is one of the key issues for the success of laser fusion to control backward SBS. Many mechanisms for the saturation of SBS have been proposed, including increasing linear Landau damping by kinetic ion heating [7, 8], frequency detuning due to particle trapping [9], coupling with higher harmonics [10, 11], two-ion decay instability [12], the creation of cavitons in plasmas [13–15] and so on. Several methods have been proposed to suppress SBS and increase the efficiency of laser coupling into fusion hohlraum such as using 2ω light [16, 17], smoothing by spectral dispersion (SSD) [3, 16], and polarization smoothing (PS) [18, 19] and so on. One of the pending questions in laser-plasma interaction is the discrepancy between the theoretically predicted reflectivity and the experimentally observed reflectivity [20]. SBS reflectivity is directly proportional to the IAW amplitude, and SBS driven IAW behaves in a nonlinear way, such as particle trapping and harmonic generation. Particle

[4] Authors to whom any correspondence should be addressed.

trapping may produce a non-Maxwellian distribution, reducing Landau damping of IAW [21] and potentially eliminating the higher IAW damping of the multi-ion species plasmas. Therefore, it is not applicable to predicting SBS reflectivity in experiment by the traditional linear growth rate and gain of SBS taking use of only the linear Landau damping, where the particle trapping is not considered and the Maxwell distribution is assumed. On the other hand, harmonic generation will dissipate the energy of fundamental IAW mode to harmonics, which will induce an efficient damping to decrease the growth rate of SBS [11, 10]. However, when the harmonic amplitude is large, the pump depletion will be obvious, thus the SBS will be saturated mainly due to pump depletion.

In this paper, we report the first demonstration that the growth rate and gain of SBS considering the nonlinear Landau damping of IAW due to particle trapping will be consistent to the simulation results better. This model considering the nonlinear Landau damping will give a good explanation of why the reflectivity in experiment or simulation was higher than the prediction of Tang model [22], where Berger *et al* [20] modeled the weakly damped data with a 'speckle-enhanced' $G = 2G(I_0)$, twice the calculated gain. This paper will show that the Landau damping will decrease with time due to particle trapping, thus the simulation data will be modeled well with gain of SBS considering reduced Landau damping due to particle trapping.

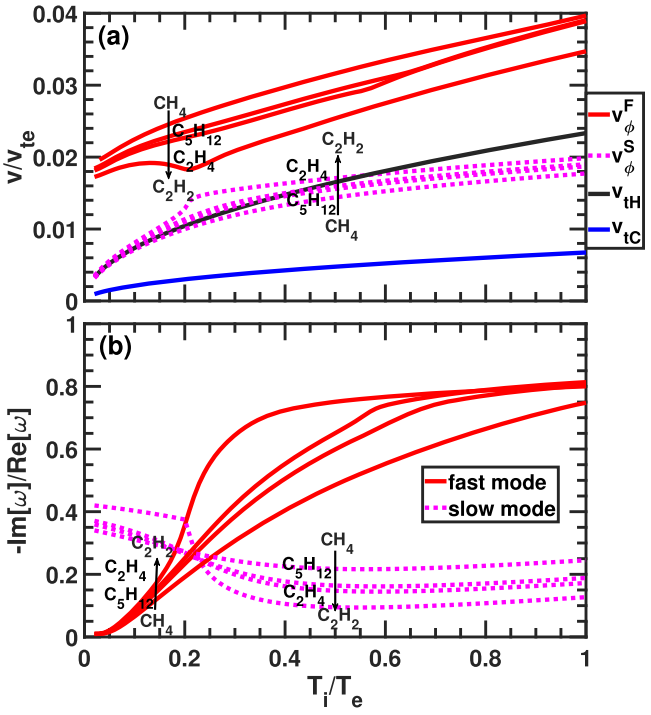

Figure 1. (a) The phase velocity and (b) the Landau damping $-\mathrm{Im}[\omega]/Re[\omega]$ of the fast mode and the slow mode in CH_4, C_5H_{12}, C_2H_4 and C_2H_2 plasmas. The arrow refers to the line from CH_4, C_5H_{12}, C_2H_4 to C_2H_2 in order. The conditions are: $T_e = 5$ keV, $n_e = 0.3n_c$ and $k_A\lambda_{De} = 0.3$.

2. Theoretical analyses

The IAW frequency is much lower than that of SBS scattering light. Thus, the wave number of IAW excited by backward SBS is $k_A\lambda_{De} \simeq 2k_0 = 2\frac{v_{te}}{c}\sqrt{n_c/n_e - 1}$, where k_0 is the wave number of pump light, $v_{te} = \sqrt{T_e/m_e}$ is the electron thermal velocity, n_e, T_e, m_e are the density, temperature and mass of the electron. Assuming fully ionized, neutral, unmagnetized plasmas, the linear dispersion relation of the ion acoustic wave in multi-ion species plasmas is given by [23–25]

$$\epsilon(\omega, k = k_A) = 1 + \sum_j \chi_j = 0, \qquad (1)$$

where χ_j is the susceptibility of particle j ($j = e, H, C$). And $\omega = Re(\omega) + i * \mathrm{Im}(\omega)$ is complex frequency. $Re(\omega)$ and $\mathrm{Im}(\omega)$ are the frequency and Landau damping of IAW. Under the condition of $T_e = 5$ keV, $n_e = 0.3n_c$, one can obtain the wave number of the IAW $k_A\lambda_{De} = 0.3$. By solving equation (1), the phase velocity $v_\phi = Re(\omega)/k$ and Landau damping $-\mathrm{Im}[\omega]/Re[\omega]$ of the fast mode and the slow mode in CH_4, C_5H_{12}, C_2H_4 and C_2H_2 are given as shown in figure 1. There exist two groups of modes called 'fast mode' and 'slow mode' in multi-ion species plasmas as shown in figure 1. Here, the fast mode refers to the mode with phase velocity larger than the thermal velocity of each species, and the slow mode refers to the mode with phase velocity close to the thermal velocity of light species ions as shown in figure 1(a). When $T_i/T_e \lesssim 0.2$, the Landau damping of the fast mode is lower than that of the slow mode, thus the fast mode is the dominated mode. When $T_i/T_e \gtrsim 0.2$, the Landau damping of the slow mode is lower than that of the fast mode, thus the slow mode is the dominated mode. The theoretical results are consistent to the observations of Froula *et al* for CH plasmas [26]. In this paper, $T_i/T_e = 0.5$ is chosen as the typical parameter since T_i approaches $T_e/2$ at the peak laser power in ICF ignition experiments [27]. With the ratio of C to H increasing, i.e. from CH_4, C_5H_{12}, C_2H_4 to C_2H_2, the Landau damping of the slow mode will decrease.

3. Numerical simulations

A one dimension Vlasov–Maxwell code [28] is used to research the SBS nonlinear growth rate and gain when the trapping and harmonic generation processes are considered. The electron temperature is $T_e = 5$ keV and electron density is $n_e = 0.3n_c$, where n_c is the critical density for the incident laser. The electron density is taken to be higher than $0.25n_c$, thus the stimulated Raman scattering [29] and two-plasmon decay instability [30, 31] are excluded. The CH_4, C_5H_{12}, C_2H_4, C_2H_2 plasmas are taken as typical examples since they are common in ICF [1, 3]. The ion temperature is $T_i = 0.5T_e$ and the slow mode will be excited and dominate in SBS. The linearly polarized pump laser intensity is $I_0 = 3 \times 10^{15}$ W cm^{-2} and the wavelength is $\lambda_0 = 0.351$ μm. And the seed light from the right boundary is with the intensity of $I_s = 10^{-4}I_0 = 3 \times 10^{11}$ W cm^{-2} and the matching frequency. The spatial scale is $[0, L_x]$ discretized with $N_x = 5000$ spatial grid points and spatial step $dx = 0.2c/\omega_0$, where ω_0 and c are

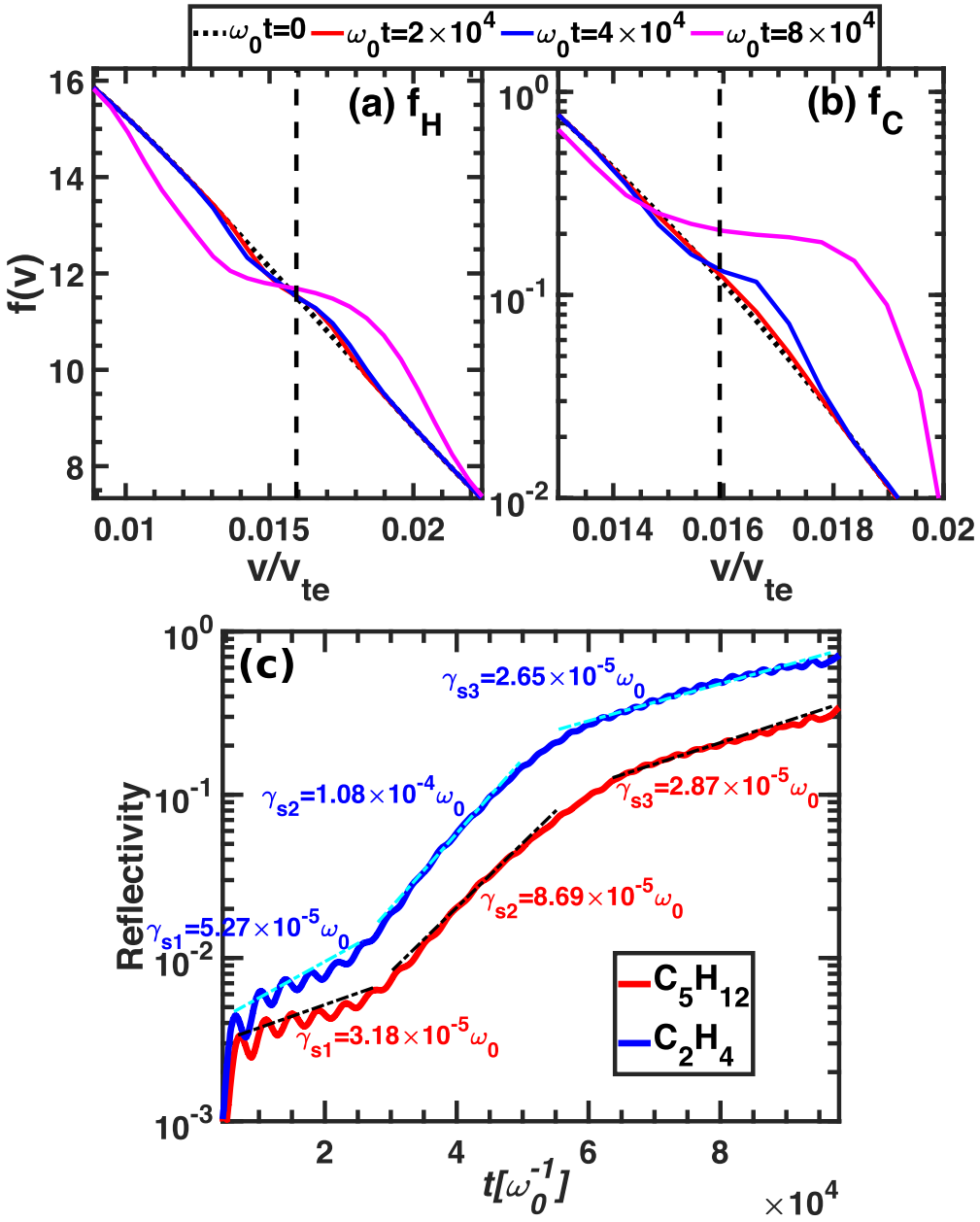

Figure 2. The velocity distribution functions averaged in the total spatial scale of (a) H ions and (b) C ions in C_2H_4 plasmas at different time points. The black dashed lines refer to the phase velocities of IAWs in C_2H_4 plasmas. (c) The growth rate of SBS reflectivity in C_5H_{12} and C_2H_4 plasmas. The conditions are: $T_e = 5$ keV, $T_i = 0.5T_e$, $n_e = 0.3n_c$ and $k_A\lambda_{De} = 0.3$ in C_2H plasmas.

the frequency of pump light and light speed in vacuum. And the spatial length is $L_x = 1000c/\omega_0 \simeq 160\lambda_0$ with $2 \times 5\%L_x$ vacuum layers and $2 \times 5\%L_x$ collision layers in the two sides of plasmas boundaries. The plasmas located at the center with density scale length $L = 0.8L_x$ are collisionless. The boundary condition of incident laser is open. The artificial strong collision layers are added into the two boundaries of plasmas, which can prevent the rebound of electrostatic waves from the boundaries and the effect of sheath field on the boundaries. The electron velocity scale $[-0.8c, 0.8c]$ and the ion (C and H) velocity scale $[-0.03c, 0.03c]$ are discretized with $2N_v+1$ ($N_v = 512$) grid points. The total simulation time is $t_{end} = 1 \times 10^5\omega_0^{-1}$ discretized with $N_t = 5 \times 10^5$ and time step $dt = 0.2\omega_0^{-1}$.

Figure 2 gives the distribution functions in C_2H_4 plasmas at different time points and the reflectivity of SBS in C_2H_4 and C_5H_{12} plasmas. Around wave phase velocity, the particles with velocity higher than wave phase velocity will transfer energy to wave, while the wave will transfer energy to the particles with velocity lower than wave phase velocity. As shown in figures 2(a) and (b), since the number of ions around the IAW phase velocity (black dashed lines in figures 2(a) and (b)) with velocity larger than the IAW phase velocity is smaller than that with velocity lower than the IAW phase velocity, more energy will transfer from ion acoustic wave to ions by wave particle interaction. Therefore, the number of energetic ions will increase and the total ion energy will increase due to particle trapping. That the wave energy

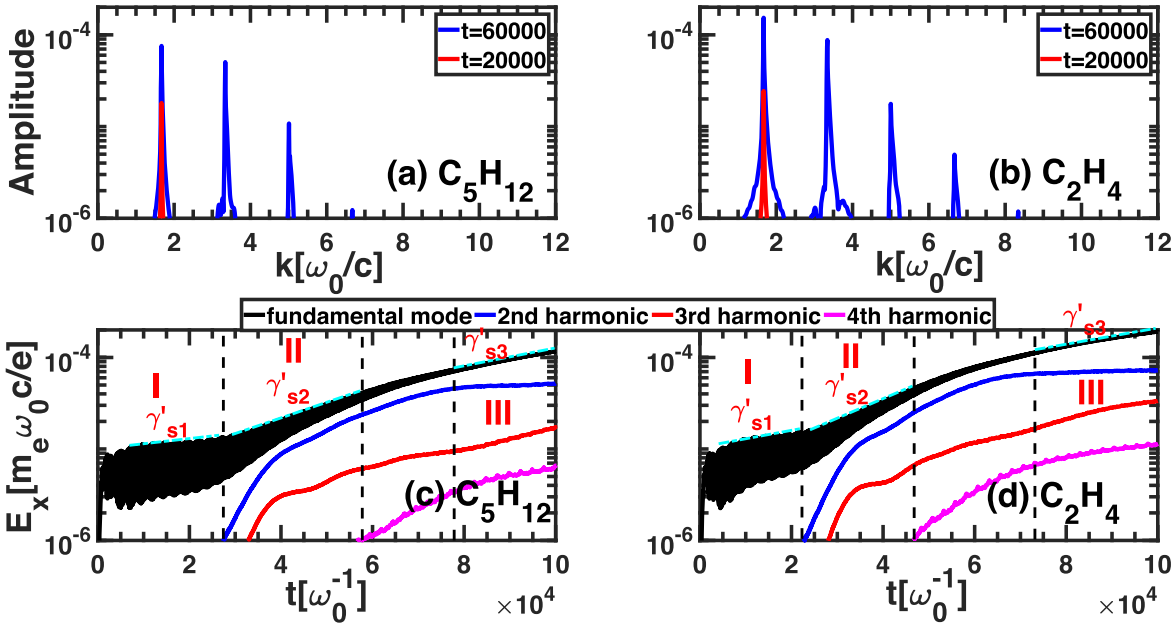

Figure 3. The wave number spectra of E_x in (a) C_5H_{12} and (b) C_2H_4 plasmas at the time of $\omega_0 t = 2 \times 10^4$ and $\omega_0 t = 6 \times 10^4$. The time evolution of fundamental mode and harmonics in (c) C_5H_{12} and (d) C_2H_4 plasmas. The condition is as the same as figure 2.

transfers to particle will lead to the damping of wave and decrease of wave energy, which is the physical picture of Landau damping. Taking C_2H_4 plasmas as an example, the absolute value of slope of distribution function around the IAW phase velocity (black dashed lines in figures 2(a) and (b)) will decrease with time due to particle trapping as shown in figures 2(a) and (b). Since the Landau damping is proportional to the slope of distribution function at the phase velocity, the Landau damping will decrease through particle trapping with time increasing. When the ion distribution nearly flats at the IAW phase velocity with time going on, for example at $t = 8 \times 10^4 \omega_0^{-1}$, the energy exchange between IAW and particles will nearly not occur, thus the Bernstein–Greene–Kruskal (BGK) modes [32] will be established. The Landau damping will be nearly zero in BGK modes. The theoretical growth rate of the SBS scattered light in homogeneous plasmas is given by [33, 34]

$$\gamma_t = \left[\frac{2\gamma_{0B}}{\sqrt{|v_{gs}|v_{gA}}} - \left(\frac{\nu_s}{|v_{gs}|} + \frac{\nu_A}{v_{gA}}\right)\right]\frac{|v_{gs}|v_{gA}}{|v_{gs}| + v_{gA}}, \tag{2}$$

where $\gamma_{0B} = \frac{1}{4}\sqrt{\frac{n_e}{n_c}}\frac{v_0}{v_{te}}\sqrt{\omega_0\omega_A}$ is the maximum temporal growth rate of SBS [20, 35], $v_0 = eA_0/m_e c$ is the electron quiver velocity. v_{gs}, v_{gA} are the group velocity of SBS scattering light and IAW. The damping rate of the backscattered light ν_s is negligible since it is much lower than the IAW Landau damping ν_A, i.e. $\nu_s \simeq 0$. The simplified expression of the nonlinear IAW Landau damping due to particle trapping is given by [36–38]

$$\nu_A(t) = \frac{\nu_A(0)}{1 + \frac{3\pi^2}{128}\int_0^t \omega_B(t)dt}, \tag{3}$$

where $\nu_A(0)$ is the linear Landau damping of IAW, $\omega_B(t) = \sqrt{eE_x(t)k_A/m_e}$ is the bounce frequency of electrons. As shown in figure 2(c), the linear growth of SBS reflectivity includes about three process: in stage I, the SBS grows with a low growth rate, the growth rate of SBS in C_5H_{12} plasmas is $\gamma_{s1} = 3.18 \times 10^{-5}\omega_0$ and that in C_2H_4 plasmas is $\gamma_{s1} = 5.27 \times 10^{-5}\omega_0$ from the start time $t_{s1} \simeq 7.5 \times 10^3 \omega_0^{-1}$. The growth rate of SBS reflectivity in C_2H_4 plasmas is higher than that in C_5H_{12} plasmas is due to the lower Landau damping in C_2H_4 plasmas. In stage II, the SBS will increase with a very large growth rate from $t_{s2} \simeq 3 \times 10^4 \omega_0^{-1}$. In C_5H_{12} plasmas, $\gamma_{s2} = 8.69 \times 10^{-5}\omega_0$ and in C_2H_4 plasmas, $\gamma_{s2} = 1.08 \times 10^{-4}\omega_0^{-1}$. In stage III, the SBS growth rate will decrease and the SBS reflectivity will saturate after stage III. Stage I and stage II can be explained by the decrease of Landau damping of IAW due to particle trapping, and stage III is as a result of pump depletion and harmonic generation, which will be discussed below in detail.

As shown in figures 3(a) and (b), at the early time such as $\omega_0 t = 2 \times 10^4$, only the fundamental mode appears and the harmonics will appear in the later time such as $\omega_0 t = 6 \times 10^4$. The frequency is proportional to the wave number of IAW, i.e. $\omega = k * c_s$, where c_s is the ion acoustic velocity and keeps constant. The wave number and frequency of fundamental mode are assumed to be k_1 and ω_1, therefore the wave numbers of the second, third and nth-order harmonics are $2k_1$, $3k_1$ and nk_1. As a result, the frequencies of the second, third and nth-order harmonics are $2\omega_1$, $3\omega_1$ and $n\omega_1$. The features of frequencies of harmonics and fundamental mode are similar to the wave numbers of harmonics and fundamental mode. The second harmonic is generated from beat of two fundamental modes. Therefore, only when the fundamental mode develops to a large amplitude, can the second harmonic develop. And in a similar fashion, the nth-order harmonic is generated from beat of the fundamental

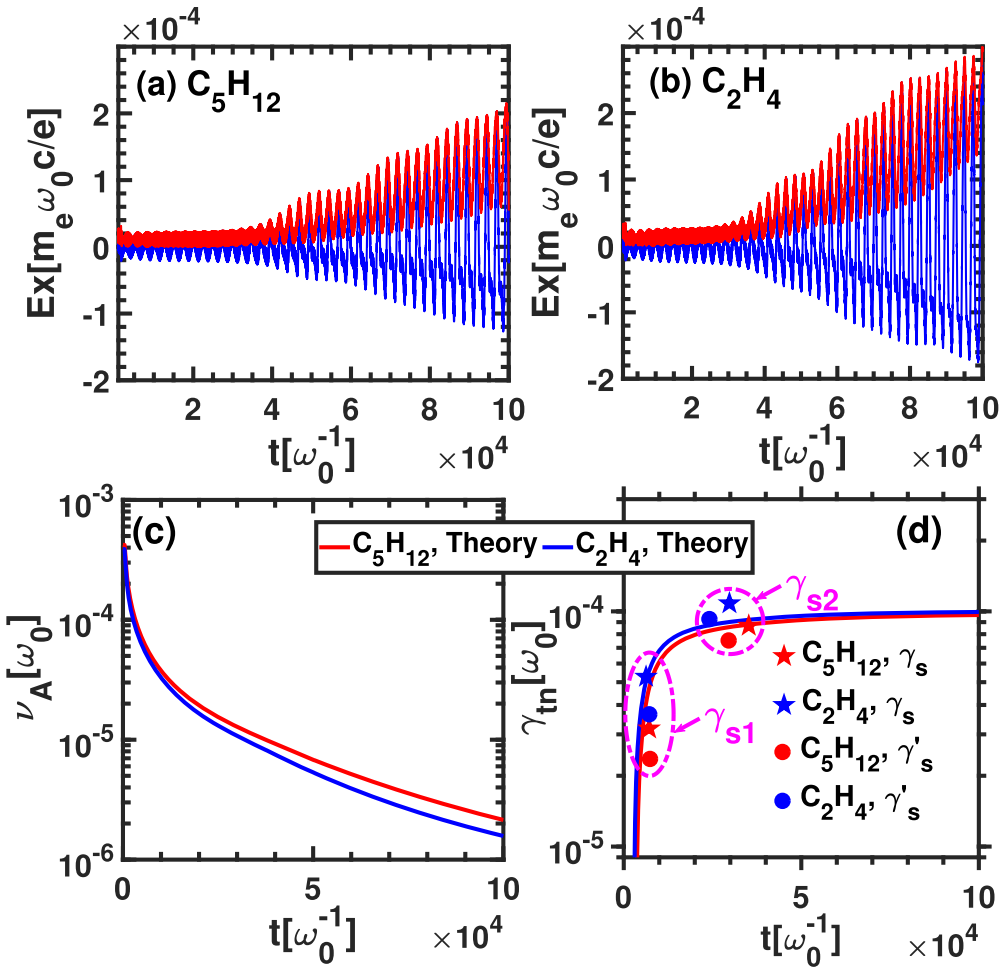

Figure 4. The time evolution and envelop of electrostatic field E_x in (a) C_5H_{12} and (b) C_2H_4 plasmas, where the blue lines are the longitudinal fields E_x and the red lines are the envelops from Hilbert transformation of E_x. The time evolution of (c) Landau damping of the slow mode and (d) growth rate considering the nonlinear Landau damping in C_5H_{12} and C_2H_4 plasmas. Where γ_s are the simulation data calculated from figure 2(c) and γ'_s are the simulation data taken from figures 3(c) and (d). The start time points of growth rates γ_{s1} and γ_{s2} are approximately chosen as the time of simulation data. The simulation results agree with theory.

mode and $(n-1)$ th-order harmonic. Therefore, only when the fundamental mode and the $(n-1)$ th-order harmonic develop to a large amplitude, can the nth-order harmonic develop. Therefore, the nth-order harmonic will develop after the $(n-1)$ th-order harmonic and the amplitude of nth-order harmonic will be usually lower than that of $(n-1)$ th-order harmonic. The harmonics will be generated sequentially. The amplitude of second harmonic ϕ_2 is proportional to square of the fundamental mode amplitude ϕ_1, i.e. $\phi_2 \propto \phi_1^2$, which is researched by Feng *et al* [25] From figures 3(c) and (d), there exist three processes of linear growth of the fundamental mode. In stage I, only the fundamental mode exists and no harmonics develop. Therefore, only the particle trapping plays a role as the nonlinear effect on the growth rate of fundamental mode. In stage II, the second and the third harmonics will increase with time, however, the amplitudes of harmonics are very low. Thus, the harmonic effect on the growth rate of $|E_x|$ is not obvious. The main nonlinear effect on growth rate of $|E_x|$ is due to particle trapping. After stage II, the nonlinear Landau damping of IAW due to particle trapping will decrease to nearly zero, as a result, the particle trapping can no longer determine the growth rate of $|E_x|$. Thus, with the harmonic increasing, the efficient damping of IAW from harmonic generation will increase and the growth rate of $|E_x|$ will be lower and lower. In stage III, the harmonics especially the second harmonic will saturate and no longer increase, thus the efficient damping of IAW due to harmonic generation will no longer increase and the growth rate of $|E_x|$ will keep constant with a low value γ'_{s3}. At the same time, SBS reflectivity reaches to a large level, thus the pump depletion will make the SBS saturation.

Figure 4 gives the time evolution of E_x, nonlinear Landau damping of slow mode ν_A and growth rate considering nonlinear Landau damping γ_{tn} in C_5H_{12} and C_2H_4 plasmas. As shown in figures 4(a) and (b), the blue solid line is the longitudinal field E_x with a oscillation period of the IAW period $\tau_A = 2\pi/\omega_A$. The red solid line is the envelop of longitudinal field E_x by Hilbert transformation. The period of high-frequency oscillation of longitudinal field is the IAW period $\tau_A = 2\pi/\omega_A$. While the period of low-frequency oscillation of the longitudinal field envelope is the bounce period $\tau_B = 2\pi/\omega_B$, which is from the particle trapping. From

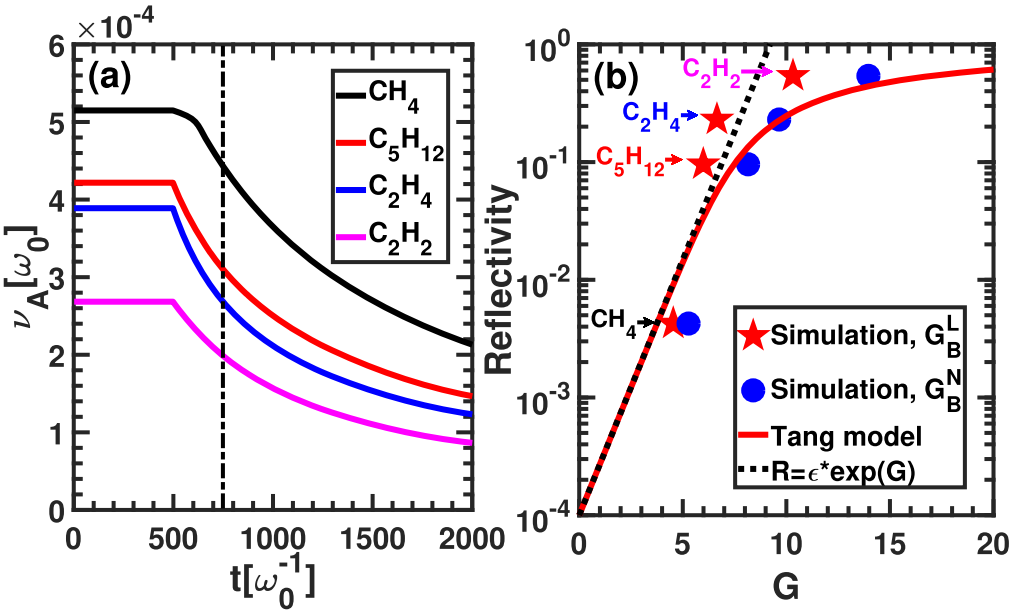

Figure 5. The early time evolution of (a) Landau damping of the slow IAW mode in different species plasmas. (b) The relation between the SBS reflectivity and SBS gain in different species plasmas. Where the Vlasov simulation data take the gain G_B^L by considering linear Landau damping (pentagram points) and the gain G_B^N considering nonlinear Landau damping at the time $\omega_0 t = 750$ (circle points).

equation (3), $\omega_B(t) = \sqrt{eE_x(t)k_A/m_e}$ is related to the amplitude of $E_x(t)$, thus, nonlinear Landau damping is a function of time. The nonlinear Landau damping ν_A is calculated from equation (3) by integral of envelop of $E_x(t)$, and growth rate γ_{tn} is calculated from equation (2) by considering nonlinear Landau damping. Comparing the growth rates of SBS reflectivity γ_{s1}, γ_{s2} calculated from figure 2(c) with the theoretical growth rate considering nonlinear Landau damping due to particle trapping, one can see that the simulation results are close to the theoretical curve. In the same way, the growth rates of $|E_x|^2$ calculated from figures 3(c) and (d) are also consistent to the theoretical curve. Where γ_s' labelled in figure 4(d) is the growth rate of energy of electrostatic field $|E_x|^2$, i.e. $\gamma_s' = [\ln(|E_x^{end}|^2) - \ln(|E_x^{start}|^2)]/(t^{end} - t^{start})$ is twice of γ_s' labelled in figures 3(c) and (d). Both the growth rate of SBS reflectivity γ_s and growth rate of the electrostatic field energy γ_s' from simulations agree well with nonlinear theoretical model as shown in figure 4(d). These results illustrate that the growth rates in stage I and stage II will be mainly affected by particle trapping. However, in stage III, the growth rate will be lower than the theoretical curve considering nonlinear Landau damping only due to particle trapping (not shown in figure 4). After stage II, particle trapping will make the Landau damping to be nearly zero, the harmonic generation will induce an efficient damping and the pump depletion will occur, which will make the growth rate lower as explained in figure 3.

Since the gain of SBS G_B is related to the Landau damping of IAW ν_A from equation (4), the Landau damping of IAW is key parameter to decide the gain of SBS. Figure 5(a) shows the variation of IAW Landau damping with time. The total simulation scale is $L_x = 1000c/\omega_0$, and the pump light and the seed light will simultaneously enter the plasmas. The pump light enters on the left boundary of plasmas and the seed light enters on the right boundary of plasmas. The pump light will meet seed light at the time of $t_0 = 500\omega_0^{-1}$. Before $t_0 = 500\omega_0^{-1}$, the pump light has not yet met the seed light and the IAW amplitude is nearly zero, thus the nonlinear effect due to particle trapping is very weak, the IAW Landau damping can be considered as the linear Landau damping ν_A^L. After $t_0 = 500\omega_0^{-1}$, the pump light will meet the seed light and the SBS or IAW will develop, the IAW Landau damping will decrease due to particle trapped by IAW. And at $t_0 = 1000\omega_0^{-1}$, the seed light will reach the left boundary of the plasmas, and $t = 750\omega_0^{-1}$ is the middle time of $[500, 1000]\omega_0^{-1}$ and can be taken as the time to calculate the IAW nonlinear Landau damping and gain considering nonlinear Landau damping. Traditionally, the gain of SBS is calculated by considering the linear Landau damping of IAW, which is shown by pentagram points in figure 5(b). We can see that the reflectivity of simulation datas will be much larger than the Tang model prediction, if the gains of simulation datas are calculated by considering linear Landau damping of IAW. Thus, the nonlinear Landau damping should be considered to calculate the gain of SBS, because the particle trapping will occur and the Landau damping will decrease with time. From equation (3), $\nu_A(t = 750\omega_0^{-1})$ in different species plasmas can be obtained as shown in figure 5(a). The gain of SBS by fluid theory is given by

$$G_B = 2\frac{\gamma_{0B}^2}{\nu_A v_{gs}}L. \tag{4}$$

Under the strong damping condition $\nu_A/\gamma_{0B} * \sqrt{v_{gs}/v_{gA}} \gg 1$ [39], one can get the Tang model [22]:

$$R(1 - R) = \varepsilon \cdot \exp[G(1 - R)] - R, \tag{5}$$

where R is the reflectivity of SBS at the left boundary, and ε is seed light at the right boundary. Pump depletion has been

considered in Tang model. If $R \ll 1$, the Tang model can be approximate to the seed amplification equation:

$$R = \varepsilon \cdot \exp(G). \tag{6}$$

The gain of SBS can be obtained by considering the linear Landau damping of IAW ν_A^L and nonlinear Landau damping of IAW at $\omega_0 t = 750$ $\nu_A(t = 750\omega_0^{-1})$, which are labelled as G_B^L and G_B^N respectively as shown in figure 5(b). When only the linear Landau damping of IAW is considered, the points by the Vlasov simulations are not consistent to the theoretical curve, especially when the gain is large, such as in C_5H_{12}, C_2H_4, C_2H_2 plasmas. However, when the nonlinear Landau damping is considered, the SBS gain from simulation will be revised to $G_B^N(t = 750\omega_0^{-1})$. And the points from Vlasov simulation are consistent to the theoretical curve of Tang model by considering nonlinear Landau damping due to particle trapping. The seed amplification model is valid only when $R \ll 1$, thus the Tang model is valid in wider scale and will be used to predict the SBS reflectivity. We can see from figure 5(b) that the reflectivities of simulation datas are much larger than the Tang model prediction if only linear IAW Landau damping is considered. This is why the SBS reflectivity in experiments is always larger than the Tang model prediction if only linear theory or the linear IAW Landau damping is considered. However, if the nonlinear IAW Landau damping is considered to calculate the SBS gain, the reflectivity of SBS will be closer to the Tang model prediction. These results may give a good explanation of why the SBS reflectivity in experiments is always larger than the Tang model prediction if only linear theory or linear IAW Landau damping is considered. Therefore, the nonlinear effect such as nonlinear Landau damping due to particle trapping should be considered to give a better explanation of SBS reflectivity in experiments.

4. Conclusions

In conclusions, growth rate and gain of SBS are proposed by considering the nonlinear Landau damping of IAW due to particle trapping. The simulation results are consistent to the theoretical analyses. Due to particle trapping, the Landau damping will decrease with time. The early SBS growth rate is mainly affected by the particle trapping, while in the later time, the harmonic generation and pump depletion will play a main role in reducing the SBS growth rate. When nonlinear Landau damping of IAW due to particle trapping is considered, the modified growth rate and gain of SBS can predict the SBS average reflectivity more accurately, which will have a wide application in the field of parametric instability in ICF experiment.

Acknowledgments

We would like to acknowledge useful discussions with C Z Xiao, Q Wang, W D Zheng and S Y Zou. This research was supported by National Postdoctoral Program for Innovative Talents (No. BX20180055), the China Postdoctoral Science Foundation (Grant No. 2018M641274), the National Natural Science Foundation of China (Grant Nos. 11 875 091, 11 875 093, 11 975 059 and 11 675 025), and Science Challenge Project, No. TZ2016005.

ORCID iDs

Q S Feng https://orcid.org/0000-0002-0757-8978
Z J Liu https://orcid.org/0000-0001-8688-692X
L Hao https://orcid.org/0000-0003-4162-5309

References

[1] He X T, Li J W, Fan Z F, Wang L F, Liu J, Lan K, Wu J F and Ye W H 2016 *Phys. Plasmas* **23** 082706
[2] Glenzer S H *et al* 2010 *Science* **327** 228
[3] Glenzer S H *et al* 2007 *Nat. Phys.* **3** 716
[4] Lan K *et al* 2016 *Matter Radiat. Extremes* **1** 8
[5] Huo W *et al* 2016 *Matter Radiat. Extremes* **1** 2
[6] Huo W Y *et al* 2016 *Phys. Rev. Lett.* **117** 025002
[7] Rambo P W, Wilks S C and Kruer W L 1997 *Phys. Rev. Lett.* **79** 83
[8] Pawley C J, Huey H E and Luhmann N C 1982 *Phys. Rev. Lett.* **49** 877
[9] Froula D H, Divol L and Glenzer S H 2002 *Phys. Rev. Lett.* **88** 105003
[10] Cohen B I, Lasinski B F, Langdon A B and Williams E A 1997 *Phys. Plasmas* **4** 956
[11] Rozmus W, Casanova M, Pesme D, Heron A and Adam J 1992 *Phys. Fluids* B **4** 576
[12] Niemann C *et al* 2004 *Phys. Rev. Lett.* **93** 045004
[13] Weber S, Riconda C and Tikhonchuk V T 2005 *Phys. Rev. Lett.* **94** 055005
[14] Weber S, Riconda C and Tikhonchuk V T 2005 *Phys. Plasmas* **12** 043101
[15] Liu Z J, He X T, Zheng C Y and Wang Y G 2009 *Phys. Plasmas* **16** 093108
[16] Niemann C *et al* 2005 *Phys. Rev. Lett.* **94** 085005
[17] Niemann C *et al* 2008 *Phys. Rev. Lett.* **100** 045002
[18] Moody J D, MacGowan B J, Rothenberg J E, Berger R L, Divol L, Glenzer S H, Kirkwood R K, Williams E A and Young P E 2001 *Phys. Rev. Lett.* **86** 2810
[19] Moody J D *et al* 2009 *Phys. Plasmas* **16** 062704
[20] Berger R L, Suter L J, Divol L, London R A, Chapman T, Froula D H, Meezan N B, Neumayer P and Glenzer S H 2015 *Phys. Rev.* E **91** 031103(R)
[21] O'Neil T 1965 *Phys. Fluids* **8** 2255
[22] Tang C L 1966 *J. Appl. Phys.* **37** 2945
[23] Williams E A, Berger R L, Drake R P, Rubenchik A M, Bauer B S, Meyerhofer D D, Gaeris A C and Johnston T W 1995 *Phys. Plasmas* **2** 129
[24] Feng Q S, Zheng C Y, Liu Z J, Xiao C Z, Wang Q and He X T 2016 *Phys. Plasmas* **23** 082106
[25] Feng Q S, Xiao C Z, Wang Q, Zheng C Y, Liu Z J, Cao L H and He X T 2016 *Phys. Rev.* E **94** 023205
[26] Froula D H, Ross J S, Divol L, Meezan N, MacKinnon A J, Wallace R and Glenzer S H 2006 *Phys. Plasmas* **13** 052704
[27] Meezan N B *et al* 2010 *Phys. Plasmas* **17** 056304
[28] Liu Z J, Zhu S P, Cao L H, Zheng C Y, He X T and Wang Y 2009 *Phys. Plasmas* **16** 112703
[29] Feng Q S, Zheng C Y, Liu Z J, Cao L H, Wang Q, Xiao C Z and He X T 2018 *Phys. Plasmas* **25** 092112

[30] Xiao C Z, Liu Z J, Wu D, Zheng C Y and He X T 2015 *Phys. Plasmas* **22** 052121
[31] Xiao C Z, Liu Z J, Zheng C Y and He X T 2016 *Phys. Plasmas* **23** 022704
[32] Bernstein B, Greene J M and Kruskal M D 1957 *Phys. Rev.* **108** 546
[33] Liu C S, Rosenbluth M N and White R B 1974 *Phys. Fluids* **17** 1211
[34] DuBois D F, Forslund D W and Williams E A 1974 *Phys. Rev. Lett.* **33** 1013
[35] Lindl J D, Amendt P, Berger R L, Glendinning S G, Glenzer S H, Haan S W, Kauffman R L, Lan-den O L and Suter L J 2004 *Phys. Plasmas* **11** 339
[36] Yampolsky N A and Fisch N J 2009 *Phys. Plasmas* **16** 072105
[37] Yampolsky N A and Fisch N J 2009 *Phys. Plasmas* **16** 072104
[38] Wang Q, Liu Z J, Zheng C Y, Xiao C Z, Feng Q S, Zhang H C and He X T 2018 *Phys. Plasmas* **25** 012708
[39] Forslund D W, Kindel J M and Lindman E L 1975 *Phys. Fluids* **18** 1002